ARMY RESEARCH LABORATORY

Extended-Range 5-in Navy Gun: Theoretical Thermal and Erosion Investigations

by Paul J. Conroy, Paul Weinacht,
Michael J. Nusca, and Kirk Rice

ARL-TR-2473 May 2001

Approved for public release; distribution is unlimited.

20010508 028

The findings in this report are not to be construed as an official Department of the Army position unless so designated by other authorized documents.

Citation of manufacturer's or trade names does not constitute an official endorsement or approval of the use thereof.

Destroy this report when it is no longer needed. Do not return it to the originator.

Army Research Laboratory
Aberdeen Proving Ground, MD 21005-5066

ARL-TR-2473 **May 2001**

Extended-Range 5-in Navy Gun: Theoretical Thermal and Erosion Investigations

Paul J. Conroy, Paul Weinacht, and Michael J. Nusca
Weapons and Materials Research Directorate, ARL

Kirk Rice
Formerly of the U.S. Naval Surface Warfare Center

Approved for public release; distribution is unlimited.

Abstract

Barrel heating and erosion concerns for the Navy are being brought to light by new extended-range munitions. These munitions have, in general, higher performance requirements and use new propellants. In light of these concerns, the following investigation was performed to determine the thermal and erosion characteristics of the current and proposed munitions. In this report, the calculation methodology governing both the thermal and erosion work is described. Six thermal scenarios were computed to compare the thermal load from various combinations of charges. Single-shot erosion predictions are presented for three charges: MK67 with NACO propellant, MK73 with M30A1 propellant, and EX167 extended-range guided munitions (ERGM) propelling charge with EX99 propellant. A fourth single-shot erosion calculation was made using the product gas-state variables and gas velocity of the MK73 charge with chemical constituents of EX99 propellant. The erosion results highlight propellant combustion product differences at the surface between the current and newer propellants. The primary conclusion is that carburization leading to iron carbide formation may be an important contributing factor for much of the material lost from the steel barrel once it is exposed through cracks or chips in the surface coating.

Table of Contents

		Page
	List of Figures	v
	List of Tables	vii
1.	**Introduction**	1
2.	**Mechanistic Descriptions**	2
2.1	Heat Transfer	2
2.2	Erosion Methodology	4
2.3	Surface Description	7
2.4	Erosion Calculations	9
2.5	Thermal Calculations	12
3.	**Conclusions**	17
4.	**References**	19
	Distribution List	21
	Report Documentation Page	29

INTENTIONALLY LEFT BLANK.

List of Figures

Figure		Page
1.	Conceptual Tube Surface Illustration	4
2.	Control Volume Description Showing Solid-Phase Dependence Upon Carbon Diffusion Depth	7
3.	Single-Shot Surface Temperatures for MK67, MK73, EX167, and MK73 With EX99 Rounds	11
4.	Single-Shot Surface Regression for MK67, MK73, EX167, and MK73 With EX99 Rounds	11
5.	Inner-Bore Residual Surface Temperatures for Scenario No. 1: 10 EX167 Rounds at 9 Rounds/min, Followed by 240 EX167 Rounds at 4 Rounds/min, Followed by 250 Rounds of MK67 at 10 Rounds/min	14
6.	Inner-Bore Residual Surface Temperatures for Scenario No. 2: 20 MK67 Rounds at 18 Rounds/min, Followed by 230 MK67 Rounds at 10 Rounds/min, Followed by 250 Rounds of EX167 at 4 Rounds/min	14
7.	Inner-Bore Residual Surface Temperatures for Scenario No. 3: 10 MK67 Rounds at 10 Rounds/min, Followed by 10 EX167 Rounds at 4 Rounds/min, Alternating Until 500 Total Rounds Are Fired	15
8.	Inner-Bore Residual Surface Temperatures for Scenario No. 4: 600 MK67 Charges at a Firing Rate of 10 Rounds/min	15
9.	Inner-Bore Residual Surface Temperatures for Scenario No. 5: 600 EX167 Charges at a Firing Rate of 4 Rounds/min	16
10.	Inner-Bore Residual Surface Temperatures for Scenario No. 6: 600 MK73 Charges at a Firing Rate of 10 Rounds/min	16

INTENTIONALLY LEFT BLANK.

List of Tables

Table		Page
1.	Modeled Propelling Charges	10
2.	Six Firing Scenarios for Thermal Considerations	12

INTENTIONALLY LEFT BLANK.

1. Introduction

The Navy's requirement for extended-range ordnance using shipboard cannons has led to the development of a new 5-in, 62-cal. MK-45, mod-4 gun system capable of firing both conventional ammunition and extended-range guided munitions (ERGM). The methods involved enabling increased range performance are higher muzzle velocity, the inclusion of a rocket in the projectile with tail fins and forward canards, and improved airframe aerodynamics. The requirement to be able to shoot the current ammunition inventory fixed the gun chamber geometry. Several other constraints limited what could be done with the gun mount, barrel, and propelling charge. The length and weight of the barrel were governed by many factors: gun mount slew rate requirements, barrel droop and whip considerations, the physical envelope available onboard ship, blast overpressure effects on ship structures, maximum trunnion loads, recoil load-handling capability, and barrel yield strength, among others. For the propelling charge, since the chamber volume was already fixed, other means were used to achieve higher muzzle velocity: increasing projectile travel due to a longer gun barrel, operating the propelling charge at a higher chamber pressure, and increasing the system chemical energy by utilizing a propellant of greater density and impetus. Unfortunately, the latter usually resulted in an increase in the adiabatic flame temperature of the propellant.

The modifications related to the propelling charge are expected to create an increased thermal load upon the gun and may result in an increase in the erosion rate. Previously, Navy guns were fatigue limited due to the extremely low adiabatic flame temperature of the Navy cool (NACO) single-based propellant. With the newer, higher energy propellant, it is expected that the gun barrel's life will be erosion limited. This report investigates the effects of candidate new charges on the system's thermal load for specific firing scenarios, as well as the erosion differences between the older and newer propelling charges. Navy 5-in gun barrels are normally plated with a 5-mil-thick layer of chrome. While this layer can afford dramatic protection from erosion, it tends to crack, flake, and peel during the first few hundred firings. In the erosion portion of this investigation, the chrome layer was assumed absent.

Historically, the propellant adiabatic flame temperature was used as an indicator of the erosivity of a propellant. Unfortunately, flame temperature was not the only factor [1, 2]. Mitigation of the erosion was a mystery, with the exception of the obvious solution of applying surface coatings or ablatives. Attempts to model erosion using first principles have been and are currently being made [3–6], although it is believed that significant additional work is required to understand the fundamental physics involved.

2. Mechanistic Descriptions

2.1 Heat Transfer. The U.S. Army Research Laboratory (ARL) XBR two-dimensional (2-D) heat-transfer/conduction code used in this report is an extension of the Veritay XBR-2D heat-transfer/conduction code [7, 8] and consists of a 2-D axisymetric implicit finite-difference heat-conduction model. Required inputs include barrel geometry and physical properties, as well as a single-round interior ballistic history of the propellant product gas velocity, pressure, and temperature.

The inner boundary condition consists of forced convective heat transfer over flat plates [8]

$$-k\frac{\partial T}{\partial r} = h\left(T_{gas} - T_{wall}\right), \tag{1}$$

where k is the conductivity, T_{gas} is the combustion product gas temperature, and T_{wall} is the wall temperature. The coefficient h is provided from a correlation of correlations [9] and given as

$$h = 0.037\frac{\mu^*}{\chi}Re^{*0.8}\frac{C_f}{C_{fi}}C_p, \tag{2}$$

where μ^* is the viscosity computed from a form of Sutherland's law, χ represents the equivalent flat-plate length to the axial position of interest, Re is the Reynolds number, $Re = \chi\rho u/\mu^*$, and C_p is the specific heat of the wall material. The compressible skin friction ratio C_f/C_{fi}, where γ is

the specific heat ratio and M is the Mach number, is given by

$$C_f/C_{fi} = \left[1 + (\gamma - 1)^2 M^2\right]^{-0.6}. \tag{3}$$

The outer boundary condition consists of both convective and radiative heat transfer and is expressed as

$$Q_w = h_{conv}(T_{wall} - T_\infty) + \sigma\varepsilon\left(T_{wall}^4 - T_\infty^4\right), \tag{4}$$

where ε is the emissivity of the wall, σ is the Boltzmann constant, and T_∞ is the temperature of the surroundings. The convection coefficient, h_{conv}, is represented by one of two models, depending on the value of the Reynolds number. For buoyant laminar flow, the convection coefficient is expressed as

$$h_{conv} = 1.32\left(\frac{T_{wall} - T_\infty}{OD}\right)^{0.25}, \tag{5}$$

for air, where OD is the outer diameter of the barrel wall. The units are accounted for in the coefficient. For buoyant turbulent cross flow in air, the convection coefficient is

$$h_{conv} = 1.2\ (T_{wall} - T_\infty)^{1/3}, \tag{6}$$

where, again, the units are accounted for in the coefficient.

This heat-transfer model has been validated with differing gun systems and differing ammunition, such as 120-mm M256 with M829 [10, 11] and M865 [10, 11]; 155 mm with M203 [8], MACS, [12] and LP zones 1–7 [13]; 25-mm Bushmaster with M919 and M791 [14]; and 27-mm caseless [8]. The results agree with the experimentally measured values.

2.2 Erosion Methodology. The erosion representation consists of three fully coupled portions, including thermal ablation and heat conduction with an iterative solution for the surface regression, independent heat and multicomponent species mass transport to the surface, and full equilibrium thermochemistry. The contributions due to mechanical wear and abrasion, however, are not included. A surface control volume treatment is also included to ensure conservation of mass of the solid-phase product species due to the solid-gas interface. The core flow gas-phase velocity, as well as state variables pressure and temperature of the gun tube from the XKTC [15] or NGEN [16] interior ballistic codes are used, as well as species data from IBBLAKE [17–19]. The thermochemistry calculation incorporates the NASA Lewis [20] thermochemical database. Primary features of the model have been described [6, 13] and are cursorily presented here.

The model, shown conceptually in Figure 1, enables the surface to heat convectively. A surface control volume is defined, and surface reactions occur, which release additional energy into the system as a surface source term. Various gas, solid, or liquid products are produced, which either remain as solids or are removed in the case of gases and liquids.

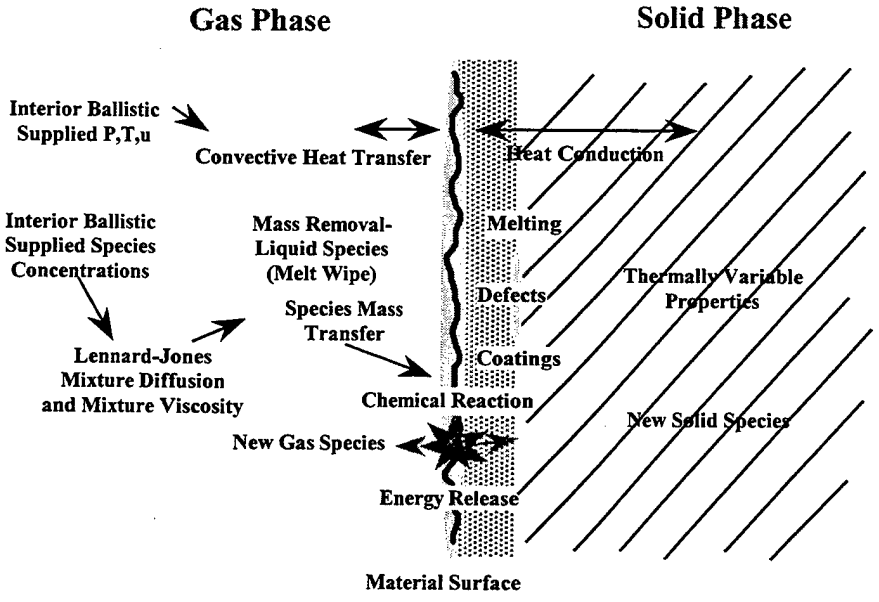

Figure 1. Conceptual Tube Surface Illustration.

The in-depth temperature response of the unablated (solid) material is modeled using the one-dimensional (1-D) heat conduction equation:

$$\rho C_p \frac{\partial T}{\partial t} = \frac{1}{r^\beta} \frac{\partial}{\partial r}\left(r^\beta k \frac{\partial T}{\partial r} \right). \tag{7}$$

By setting $\beta = 0$ or $\beta = 1$, the planar or axisymmetric form of the governing equation can be obtained. The relevant material properties are density,ρ; specific heat, C_p; and conductivity, k. The conductivity and specific heat vary with temperature.

The surface energy balance, while gross melting is not occurring, includes the same convective surface heat input used in the thermal calculations, along with the possible contribution due to the surface reaction (shown in equation 8). This source term is balanced with the energy conducted through the material:

$$h\left(T_{gas} - T_{wall}\right) = -k\frac{\partial T}{\partial r} + Source. \tag{8}$$

However, when the system is melting, the energy balance includes the fixed surface temperature condition, as well as the unknown surface location. The surface temperature cannot rise beyond the specified melting value because any additional energy is applied to the material-phase transition (melting) as shown:

$$T_{wall} = T_{melt}, \quad \rho L\frac{\partial s}{\partial t} = h\left(T_{gas} - T_{wall}\right) + k\frac{\partial T}{\partial r} - Source. \tag{9}$$

Prior to the onset of melting, the governing equations and boundary conditions are linear, and solutions are obtained in a direct (noniterative) fashion. During the melting process, the equations become nonlinear since the computational domain dimensions are coupled to the regression rate. An iterative approach is utilized during melting to address the nonlinearity. Because the boundary of the computational domain moves during the erosion event, a

transformed version of the governing equation is employed. This allows the equations to be solved in a fixed computational space, even though the physical boundary is moving. A generalized transformation between the computational coordinate, ξ, and the physical coordinate, r, is utilized, as shown in the transformed equations:

$$\rho C_p \left(\frac{\partial T}{\partial t} + \xi_t \frac{\partial T}{\partial \xi} \right) = \frac{1}{r} \xi_r \frac{\partial}{\partial \xi} \left(r k_r \frac{\partial T}{\partial \xi} \right),$$

$$\xi_t = \frac{-r_t}{r_\xi} \equiv \frac{\partial r}{\partial t} \frac{\partial \xi}{\partial r},$$

and

$$\xi_r = \frac{1}{r_\xi} \equiv \frac{\partial \xi}{\partial r}. \tag{10}$$

In this form, the nonlinear nature of the governing equation produced by the moving boundary is evident because the metric terms, ξ_r and ξ_t, are not constant and are dependent on the erosion rate when the grid is moving. This methodology compares very well to the semi-analytical solutions of Landau in test cases [20].

The species mass transport to the surface from the core flow of the propellant product gases is assumed frozen and is provided through a concentration potential $\varphi_{i\ core\ -\ flow} - \varphi_{i\ wall}$ for each species i, and a mass transport coefficient h_m derived from Sherwood number correlations integrated over space and time [6]:

$$Mass_i = \iint h_m \left(\varphi_{i\ core\ -\ flow} - \varphi_{i\ wall} \right) dA\, dt. \tag{11}$$

The surface control volume reaction is governed by equilibrium kinetics because the actual reactions and rates are not well known at this time. Equilibrium chemical processes are considered to dominate whenever the characteristic time for a fluid element to traverse the flow field of interest is much longer than the characteristic time for chemical reactions to approach

equilibrium. As the pressure and temperature increase, the molecular collision frequency and energy per collision increases, leading to smaller characteristic chemical times, and the chemical processes approach equilibrium.

The condition for chemical equilibrium may be stated as the minimization of the Gibbs free energy [21]. For a mixture of N species (e.g., atoms or molecules) with the number of moles of species denoted as n_i, the Gibbs free energy per mole of mixture is given in terms of the Gibbs free energy of the individual species, g_i; the internal energy, e; the temperature, T; the entropy, s; the pressure, p; and the specific volume, v:

$$G = \sum_{i=1}^{N} n_i g_i = e - Ts + pv. \tag{12}$$

2.3 Surface Description. The full equilibrium control volume approach, as shown in Figure 2, results in many product mass fractions that are physically impossible due to the constraints of diffusion into the solid phase. Mainly, the carbon that results from CO and/or CO_2 breakdown will react with as much iron as possible to form Fe_3C if permitted. To treat this deficiency, the amount of carbon available for a reaction with the steel is diffusion limited.

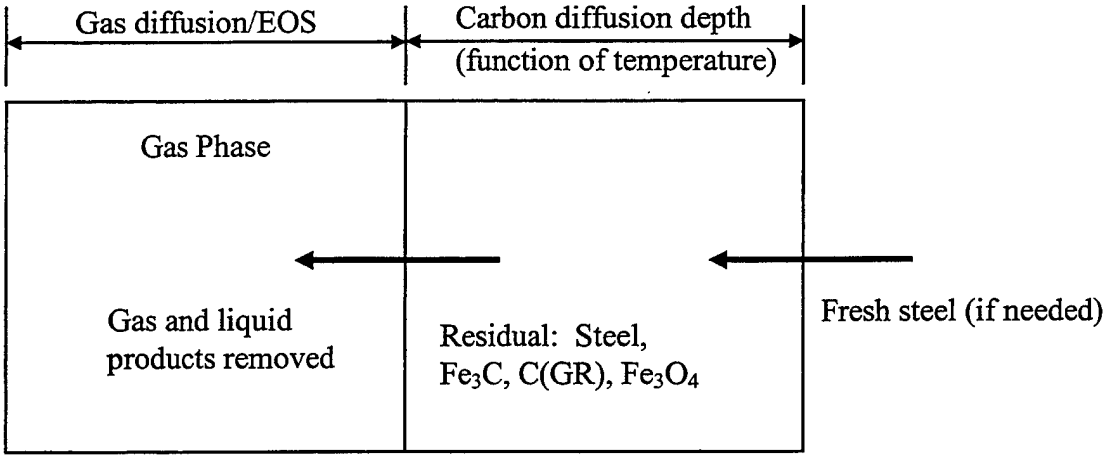

Figure 2. Control Volume Description Showing Solid-Phase Dependence Upon Carbon Diffusion Depth.

A surface exposed to a carbon concentration G per unit surface area for a specified length of time t has a carbon concentration $C(x)$ at a specified depth of x given by the following relationship:

$$C(x) = \frac{G}{\sqrt{\pi D t}} e^{\frac{-x^2}{4Dt}}, \tag{13}$$

where D is the diffusion coefficient over the α and γ phases (body-centered cubic [BCC] and face-centered cubic [FCC] lattice structure, respectively). The diffusion of carbon into α iron ($T < 1{,}118$ °C) is given by the following function in *Smithells Metals Reference Handbook* [22] in square centimeters per second, were R_u is the universal gas constant in (kilo-calories per mole per Kelvin):

$$D = 0.008e^{\frac{-19.8}{R_u T}} + 2.2e^{\frac{-29.3}{R_u T}}, \tag{14}$$

while the diffusion of carbon into γ iron ($T < 1{,}300$ °C) is provided by

$$D = 0.36e^{\frac{-36}{R_u T}}. \tag{15}$$

To find the total amount of carbon that has diffused in time t, the concentration function can be integrated and has an error function solution as

$$\int_0^x C(x)\,dx = \frac{G}{\sqrt{\pi D t_0}} \int_0^x e^{\frac{-x^2}{4Dt}}\,dx = G(erf(x)). \tag{16}$$

Integrating the concentration profile to the maximum depth to which material can diffuse in time t provides the carbon diffused into the material over the time period. To treat the reactant products from the full equilibrium calculation, a subset reaction is created consisting of the

carbon, iron (α) and iron (γ), and iron carbide. The total carbon available for reaction is equal to the diffused carbon plus the residual carbon in solid from the original steel or carbon in the form of iron carbide, as well as the possible carbon on the surface:

$$C(GR) + \mathrm{Fe}(\alpha) + \mathrm{Fe}(\gamma) \leftrightarrow \mathrm{Fe_3C}, \tag{17}$$

where Fe(α) or Fe(γ) are supplied as fresh material as needed, depending upon the control volume temperature. The product carbon, in the solid portion of the control volume, $C(GR)$, and Fe_3C from the previous time step are retained as residuals and reintroduced as reactants in the next time step unless the surface temperature is over the melting point of Fe_3C, in which case the carbide is removed. If there is no excess carbon, then Fe(α) or Fe(γ), depending on the temperature, is carried over to the next time step. Once the post-equilibrium calculation is made, the final energy change in the control volume is recomputed and the amount attributable to the residual solids is accounted for as the surface energy source term. Oxide formations are treated similarly.

2.4 Erosion Calculations. Four Navy propelling charges were modeled, as presented in Table 1. The first three (EX167, MK73, and MK67) have been fired in the cannon specified. The fourth round (EX9973) is a numerical experiment of a hypothetical propelling charge using EX99 propellant with a MK92 projectile in the 5-in/62-cal. gun, with matching ballistics characteristics to the MK73 charge in the same gun. This charge provides an interesting comparison to the standard MK73 charge since the ballistic performance, total system chemical energy, and propellant flame temperatures are very similar, while the concentrations of certain propellant combustion species differ substantially. Namely, for the M30A1, the principle combustion product is N_2, while for the EX99, it is CO. Normally, the MK73 charge includes a TiO_2/wax wear-reducing liner that tends to reduce the heat transfer to the barrel somewhat; however, the liner was not included in this investigation.

Please note that the caliber of the cannon includes between 35 and 40 in of chamber, so the travel is not the length of the tube. Each of these rounds was modeled using XKTC and

Table 1. Modeled Propelling Charges

Propelling Charge	Propellant/ Weight (lb)	Adiabatic Flame Temp. (K)	Projectile/ Weight (lb)	Peak IB Pressure (psi)	Muzzle Velocity (ft/s)	Cannon (in/cal.)
EX167	EX99/26.50	~3,010	ERGM/110	67	2,812	5/62
MK73	M30A1/21.26	~3,040	MK109/68.2	55	3,098	5/62
MK67	NACO/20.78	~2,285	MK92/70.0	52	2,791	5/62
EX9973 Num. Exp.	EX99/20.00	~3,010	MK109/68.2	54	3,105	5/62

IBBLAKE to obtain gas state and velocity data, as well as the thermochemical constituents for each charge.

The single-shot inner surface peak temperatures are presented in Figure 3 for the four rounds modeled in Table 1. As expected, the EX167 charge with the EX99 propellant had the highest inner surface temperature of about 1,625 K at 43 in from the rear face of the tube (RFT), while the MK67 propelling charge with the NACO propellant had the lowest inner surface temperature of about 1,210 K at 40.9 in from RFT. The surface temperatures for both the MK73 and altered propellant MK73 were between the MK67 and EX99 temperatures, with a peak of about 1,575 K at 40.9 in from RFT. Note that these wall surface temperatures are only short-lived transients that decay to much lower "residual" temperatures within seconds of the firing as the energy diffuses into the gun tube.

The erosion predictions in Figure 4 highlight not only the surface temperature effects on erosion but also the propellant combustion product differences at the bore surface for each of the three propellants. The results are fairly consistent with the rule of thumb concerning barrel surface and adiabatic flame temperatures, where the EX167, MK73, and MK67 propelling charges exhibit a decreasing trend in material lost. Perhaps the most interesting result occurred when the chemistry from a matching pressure and velocity EX99 charge of the MK73 charge was placed into the MK73 erosion calculation. Figure 4 demonstrates an increase in erosion of about 15%, not accounted for through surface temperature changes, but rather through species

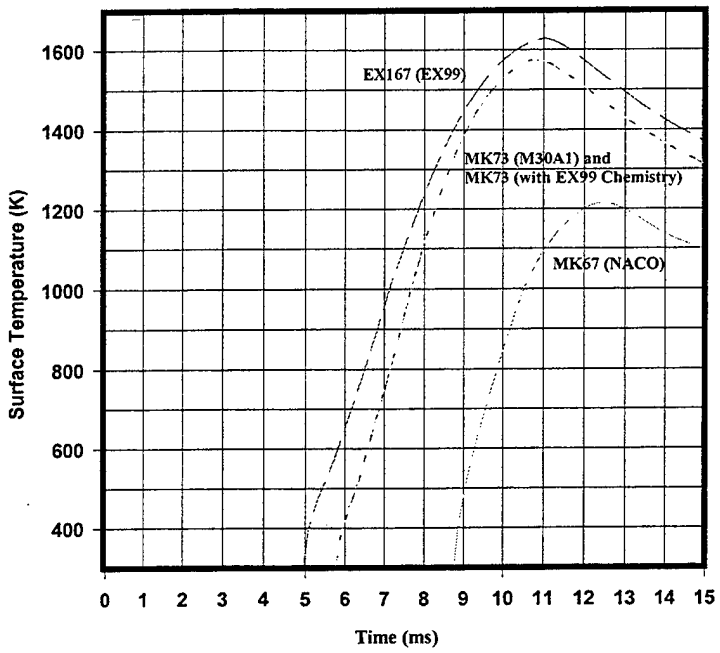

Figure 3. Single-Shot Surface Temperatures for MK67, MK73, EX167, and MK73 With EX99 Rounds. (All Are at 40.9 in From RFT, Except the EX167, Which Is at 43 in.)

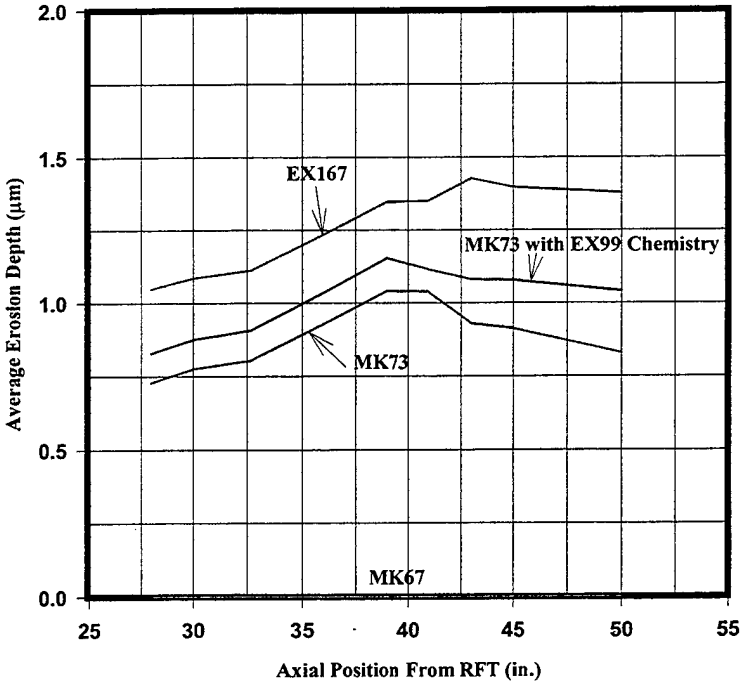

Figure 4. Single-Shot Surface Regression for MK67, MK73, EX167, and MK73 With EX99 Rounds.

concentration differences in the combustion products of EX99 propellant and M30A1 propellant. Given that none of these charges cause the surface to exhibit gross melting of the original gun steel material (i.e., the bore temperature never reaches the melt temperature), the mechanism described for the material loss (i.e., removal of the carbide formed) is controlling the erosion rate.

2.5 Thermal Calculations. For the thermal scenario investigations, six firing scenarios are specified in Table 2 with a mix of rounds. Each scenario was computed assuming that the charge case was nonexistent, and the rounds are ordered as shown in the table. The EX167 propelling charge must be double-rammed with the long rocket-assisted projectile rammed in the first cycle, and the propelling charge must be rammed separately in the second cycle. Maximum firing rate for these rounds that are in the ready service drum is about 9 rounds/min. After this supply is depleted, rounds must be taken from the magazine and hand loaded into the ready-service drum. This reduces the effective firing rate for following rounds to about 4 rounds/min.

Table 2. Six Firing Scenarios for Thermal Considerations

Scenario No.	Type of Prop. Charge	No. of Rounds	Firing Rate (rounds/min)	Round Location
1	EX167	10	9	In ready-service drum
	EX167	240	4	From storage
	MK67	250	10	From storage
2	MK67	20	18	In ready-service drum
	MK67	230	10	From storage
	EX167	250	4	From storage
3	MK67	10	10	From storage
	EX167	10	4	From storage
Continue sustained firing, alternating propelling charge type every 10 rounds until 250 of each charge has been fired.				
4	MK 67	600	10	From storage
5	EX 167	600	4	From storage
6	MK 73	600	10	From storage

The MK67 and MK73 propellant charges are single-rammed, so the maximum firing rate for rounds that are in the ready service drum is 18 rounds/min. After this supply is depleted, rounds must be taken from the magazine and hand loaded into the ready service drum. This reduces the effective firing rate for following rounds to about 10 rounds/min.

Scenario nos. 1–3 involve mixed ammunition and mixed firing rates presented in Figures 5–7. Figure 5 demonstrates the effect of firing rate on temperature increase. As the firing rate changes from 9 rounds/min to 4 rounds/min, the temperature quickly responds by dropping a little, producing a small spike or sawtooth. When the firing rate is once again increased to 10 rounds/min, the temperature profile responds again by jumping up about 20 K, until settling into a new heating profile. The peak temperatures experienced at the end of this scenario are about 1,025 K. The temperature history for scenario no. 2 shown in Figure 6 is somewhat the inverse of scenario no. 1 in that the firing rate is more rapid at the beginning and then slows down. This gives the energy more time to soak through the cannon and assist in removing the energy in external convection by having the external temperature difference higher for a longer period of time; thus, the final temperatures are slightly lower than scenario no. 1 at about 1,000 K. Scenario no. 3 involves an even mixing of the firing rates and charges. It also produces what appears to be the worst of the first three scenarios, with a final temperature of between 1,150 K and 1,250 K. The sawtooth effect presented is also seen in scenario no. 1 during the change from 4 rounds/min to 10 rounds/min, with a similar jump in temperature. This effect is coupled to the uniformity of the temperature throughout the barrel. The radial temperature profile does not settle into a steady increase in temperature (i.e., a top-hat profile) for scenario no. 3, but rather is continuously driven to higher differentials between the outer and inner temperatures, thus resulting in higher inner surface temperatures.

The results of the calculations for scenario nos. 4–6 are presented in Figures 8–10. The inner surface temperature for the nominal MK67 NACO charge rises over the 600 rounds, at 10 rounds/min, to about 1,000 K in Figure 8. Figure 9 shows that the temperature of the cannon rises to about 1,050 K at the case mouth for the EX167 charges. Figure 3 shows that the single-shot peak temperature is highest for the EX167 charge (EX99 propellant). An explanation for

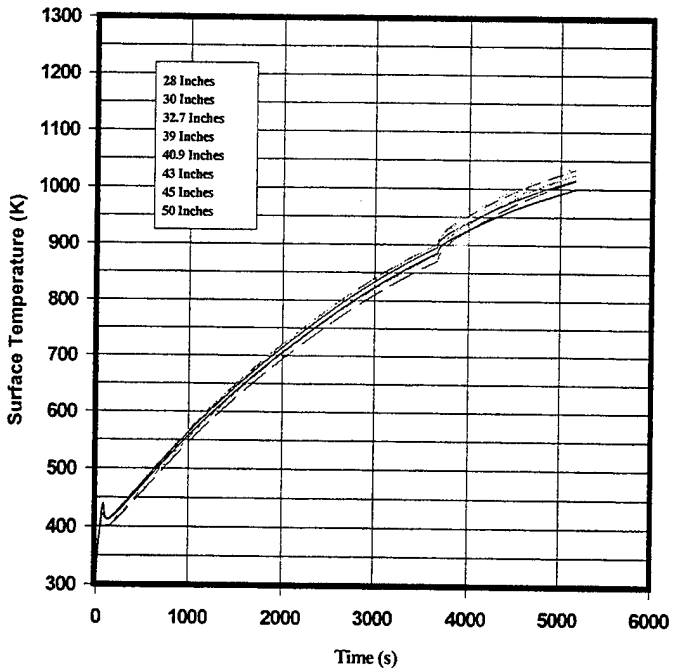

Figure 5. **Inner-Bore Residual Surface Temperatures for Scenario No. 1: 10 EX167 Rounds at 9 Rounds/min, Followed by 240 EX167 Rounds at 4 Rounds/min, Followed by 250 Rounds of MK67 at 10 Rounds/min.**

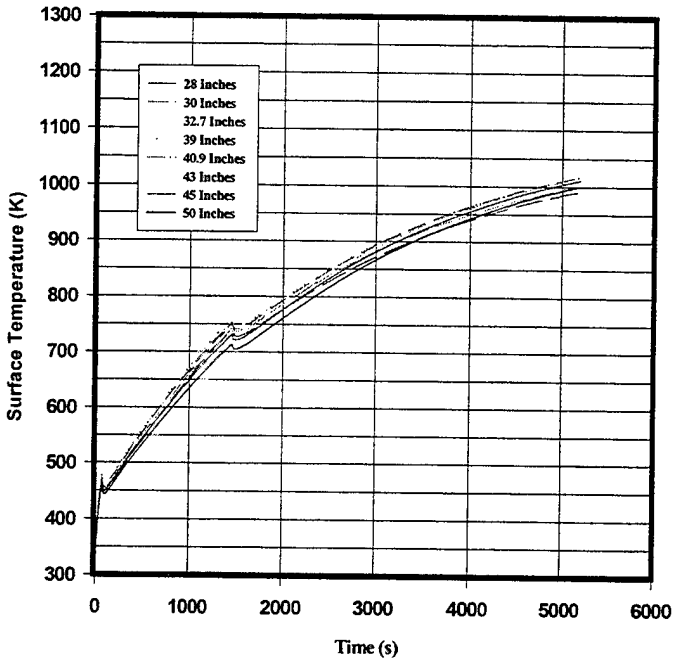

Figure 6. **Inner-Bore Residual Surface Temperatures for Scenario No. 2: 20 MK67 Rounds at 18 Rounds/min, Followed by 230 MK67 Rounds at 10 Rounds/min, Followed by 250 Rounds of EX167 at 4 Rounds/min.**

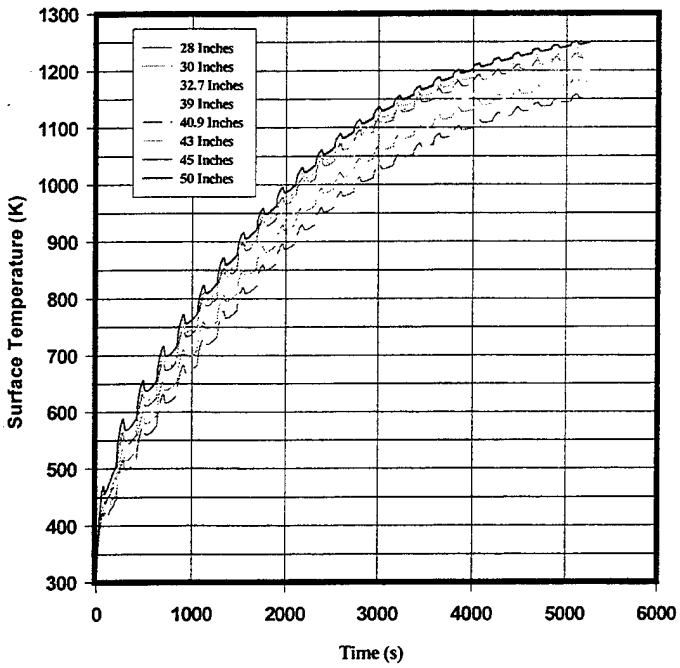

Figure 7. Inner-Bore Residual Surface Temperatures for Scenario No. 3: 10 MK67 Rounds at 10 Rounds/min, Followed by 10 EX167 Rounds at 4 Rounds/min, Alternating Until 500 Total Rounds Are Fired.

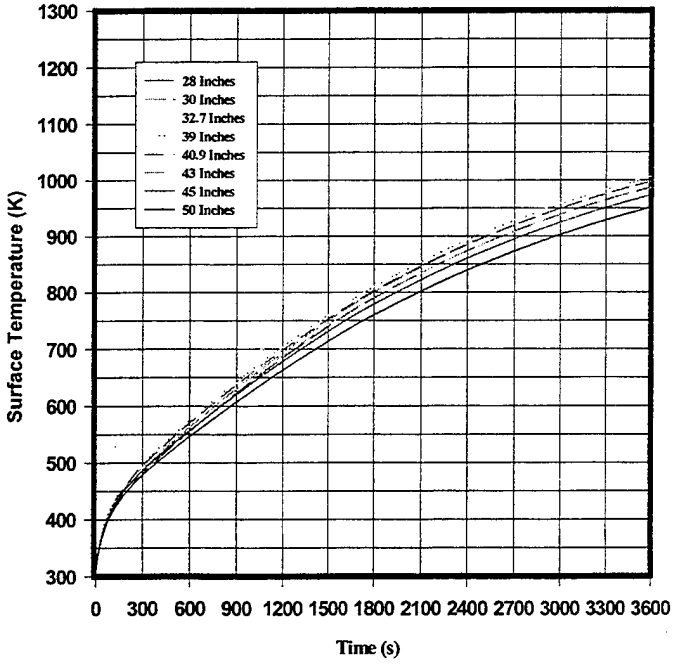

Figure 8. Inner-Bore Residual Surface Temperatures for Scenario No. 4: 600 MK67 Charges at a Firing Rate of 10 Rounds/min.

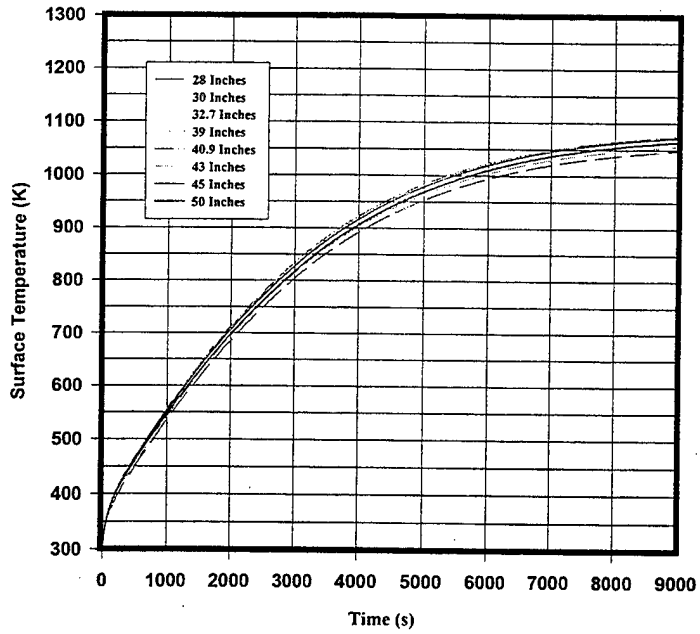

Figure 9. Inner-Bore Residual Surface Temperatures for Scenario No. 5: 600 EX167 Charges at a Firing Rate of 4 Rounds/min.

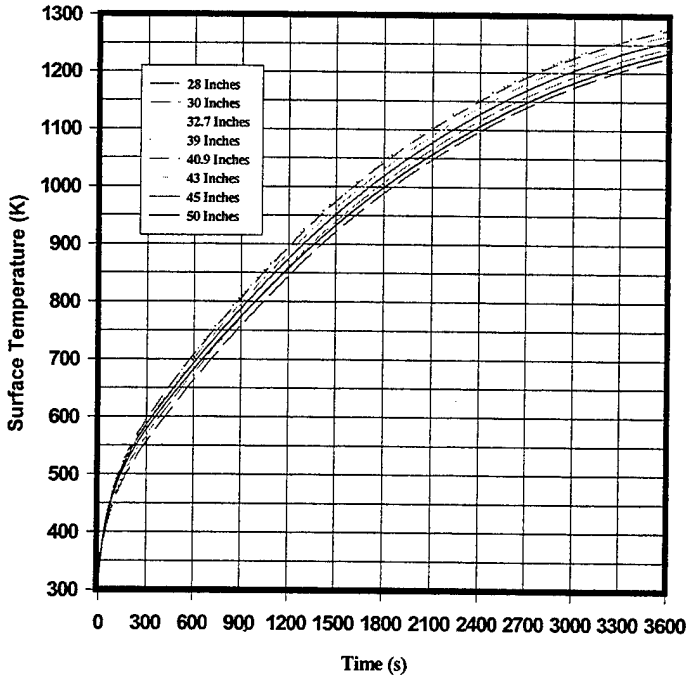

Figure 10. Inner-Bore Residual Surface Temperatures for Scenario No. 6: 600 MK73 Charges at a Firing Rate of 10 Rounds/min.

why the higher flame temperature EX99 propellant and the low-temperature NACO propellant produce very nearly the same peak residual bore temperatures in the firing scenarios is that the reduced firing rate of the EX167 round due to double ramming reduces the overall thermal burden on the cannon. Figure 10 presents the MK73 M30A1 propellant scenario of 600 rounds at 10 rounds/min. Of these three scenarios, this one has the highest temperature in the region of the case mouth, about 1,250 K.

Any potential discrepancy between these computed scenarios and existing experimental data is most likely due to potential inaccuracies in the external heat-transfer coefficient. The coefficients chosen may not be applicable when the external temperatures becomes as high, as in these scenarios under these extreme firing and thermal-loading conditions. Also, it must be noted that, even at these high temperatures, there will still be a temperature gradient from the inner wall temperature plotted herein to the outer wall temperatures measured elsewhere over a long firing scenario.

3. Conclusions

The primary conclusion concerning the erosion potential for the charges is that, although the flame temperature is about the same for the EX99 propellant and M30A1 propellants, their erosivity appears to be much different because of the product species. In M30A1, the primary product species is N_2, while EX99 has carbon monoxide as the principal product species. Carbon monoxide degenerates on the surface and is the principle source of carbon for iron carbide formation. These results stress the importance of developing an effective wear-reducing agent for the EX167 propelling charge. The Navy is currently evaluating such agents in the form of conventional TiO_2/wax wear-reducing liners and ablative paste.

The predominate erosion mechanism proposed states that carburization leading to iron carbide formation may be an important contributing factor for much of the material lost from the steel barrel once it is exposed through cracks or chips in the surface coating. Iron carbide melts at about 1,423 K as opposed to gun steels, which typically melt above 1,700 K.

The EX167 round may not load the cannon thermally more than it already is with the MK67 NACO charge. The MK73 charge loads the cannon much more severely then either of the other two.

The results obtained in this investigation have not been validated experimentally. It is unlikely that they can be, as it becomes cost-prohibitive to manufacture components and conduct a test of the magnitude required to study these effects.

Future work may focus on adding species chemistries to simulate the effect of an ablative layer that has been deposited on the inner bore surface of the gun barrel.

4. References

1. Ward, J. R., T. L. Brosseau, R. P. Kaste, I. C. Stobie, and B. Bensinger. "Erosivity of LOVA Propellants." ARBRL-TR-02368, U.S. Army Ballistic Research Laboratory, Aberdeen Proving Ground, MD, September 1981.

2. Caveny, L. H. "Steel Erosion Produced by Double Base, Triple Base, and RDX Composite Propellants of Various Flame Temperatures." ARLCD-CR-80016, Picatinny Arsenal, NJ, October 1980.

3. Evans, M. R. "User's Manual for Transient Boundary Layer Integral Matrix Procedure TBLIMP." Aerotherm UM-74-55, Prepared for the Naval Ordnance Station, Indian Head, MD, October 1974.

4. Dunn, S., D. Coats, G. Nickerson, S. Sopok, P. O'Hara, and G. A. Pflegle. "Unified Computer Model for Predicting Thermochemical Erosion in Gun Barrels." AIAA 95-2440, Proceedings of 31st AIAA/ASME/SAE/ASEE Joint Propulsion Conference, July 1995.

5. Weinacht, P., and P. J. Conroy. "A Numerical Method for Predicting Thermal Erosion in Gun Tubes." ARL-TR-1156, U.S. Army Research Laboratory, Aberdeen Proving Ground, MD, July 1996.

6. Conroy, P. J., P. Weinacht, and M. J. Nusca. "120-mm Gun Tube Erosion Including Surface Chemistry Effects." ARL-TR-152, U.S. Army Research Laboratory, Aberdeen Proving Ground, MD, October 1997.

7. Crickenberger, A. B., R. L. Talley, and J. Q. Tally. "Modifications to the XBR-2D Heat Conduction Code." ARL-CR-126, U.S. Army Research Laboratory, Aberdeen Proving Ground, MD, April 1994.

8. Conroy, P. J. "Gun Tube Heating." BRL-TR-3300, U.S. Army Ballistic Research Laboratory, Aberdeen Proving Ground, MD, December 1991.

9. Stratford, B. S., and G. S. Beavers. "The Calculation of the Compressible Turbulent Boundary Layer in Arbitrary Pressure Gradient - A Correlation of Certain Previous Methods." Aeronautical Research Council R&M, No. 3207, 1961.

10. Conroy, P. J., M. L. Bundy, and J. L. Kennedy. "Experimental and Simulated Bore Surface Temperatures for 120-mm Ammunition." ARL-TR-770, U.S. Army Research Laboratory, Aberdeen Proving Ground, MD, June 1995.

11. Bundy, M. L., P. J. Conroy, and J. L. Kennedy. "Experimental and Simulated Bore Surface Temperatures for 120-mm Ammunition." *Journal of Defense Science,* October 1996.

12. Keller, G. E., A. W. Horst, P. J. Conroy, and T. P. Coffee. "The Influence of Propulsion Technique and Firing Rate on Thermal Management Problems in Large-Caliber Guns." ARL-TR-130, U.S. Army Research Laboratory, Aberdeen Proving Ground, MD, May 1993.

13. Conroy, P. J., T. P. Coffee, and G. E. Keller. "RLPG Chamber Heating." ARL-MR-179, U.S. Army Research Laboratory, Aberdeen Proving Ground, MD, September 1994.

14. Conroy, P. J., P. Weinacht, and M. J. Nusca. "The U.S. Army Research Laboratory Gun Tube Erosion Code (ATEC) Applied to Systems (Point Studies)." U.S. Army Research Laboratory, Aberdeen Proving Ground, MD, in review.

15. Gough, P. S. "The XNOVAKTC Code." BRL-CR-627, U.S. Army Ballistic Research Laboratory, Aberdeen Proving Ground, MD, February 1990.

16. Nusca, M. J. "Investigation of Solid Propellant Gun Systems Using the Next-Generation Interior Ballistics Code." CPIA Pub. No. 620, vol. 1, pp. 279–292, October 1994.

17. Freedman, E. "BLAKE - A Thermodynamic Code Based on Tiger: Users' Guide and Manual." ARBRL-TR-02411, U.S. Army Ballistic Research Laboratory, Aberdeen Proving Ground, MD, July 1982.

18. Anderson, R. D., and K. D. Fickie. "IBHVG2- A Users Guide." BRL-TR-2829, U.S. Army Ballistic Research Laboratory, Aberdeen Proving Ground, MD, July 1987.

19. Janke, P. J., J. A. Dyvik, and C. L. Marksberry. "Electrothermo-Chemical Propellant Extensions to the IBHVG2 Interior Ballistics Simulation: Model Development and Validation." CPIA Publication No. 620, vol. 3, pp. 171–181, October 1994.

20. Landau, H. G. "Heating Conduction in a Melting Solid." *Quarterly of Applied Mathematics,* vol. 8, pp. 81–94, 1950.

21. Gordon, S., and B. J. McBride. "Computer Program for Calculation of Complex Chemical Equilibrium Compositions, Rocket Performance, Incident and Reflected Shocks, and Chapman-Jouget Detonations." NASA SP-273, NASA Lewis, Cleveland, OH, 1971.

22. Brandes, E. A. *Smithells Metals Reference Handbook.* Sixth Edition, Boston, MA: Butterworth and Company, 1983.

NO. OF COPIES	ORGANIZATION
2	DEFENSE TECHNICAL INFORMATION CENTER DTIC OCA 8725 JOHN J KINGMAN RD STE 0944 FT BELVOIR VA 22060-6218
1	HQDA DAMO FDT 400 ARMY PENTAGON WASHINGTON DC 20310-0460
1	OSD OUSD(A&T)/ODDR&E(R) DR R J TREW 3800 DEFENSE PENTAGON WASHINGTON DC 20301-3800
1	COMMANDING GENERAL US ARMY MATERIEL CMD AMCRDA TF 5001 EISENHOWER AVE ALEXANDRIA VA 22333-0001
1	INST FOR ADVNCD TCHNLGY THE UNIV OF TEXAS AT AUSTIN 3925 W BRAKER LN STE 400 AUSTIN TX 78759-5316
1	DARPA SPECIAL PROJECTS OFFICE J CARLINI 3701 N FAIRFAX DR ARLINGTON VA 22203-1714
1	US MILITARY ACADEMY MATH SCI CTR EXCELLENCE MADN MATH MAJ HUBER THAYER HALL WEST POINT NY 10996-1786
1	DIRECTOR US ARMY RESEARCH LAB AMSRL D DR D SMITH 2800 POWDER MILL RD ADELPHI MD 20783-1197

NO. OF COPIES	ORGANIZATION
1	DIRECTOR US ARMY RESEARCH LAB AMSRL CI AI R 2800 POWDER MILL RD ADELPHI MD 20783-1197
3	DIRECTOR US ARMY RESEARCH LAB AMSRL CI LL 2800 POWDER MILL RD ADELPHI MD 20783-1197
3	DIRECTOR US ARMY RESEARCH LAB AMSRL CI AP 2800 POWDER MILL RD ADELPHI MD 20783-1197
	ABERDEEN PROVING GROUND
2	DIR USARL AMSRL CI LP (BLDG 305)

NO. OF COPIES	ORGANIZATION
1	HQDA DIR R&D SAAL TR W MORRISON SUITE 9800 2511 JEFFERSON DAVIS HWY ARLINGTON VA 22201
1	HQS US ARMY MATERIEL CMD AMCICP AD 5001 EISENHOWER AVE ALEXANDRIA VA 22331-0001
1	US ARMY BMDS CMD ADVANCED TECHLGY CTR PO BOX 1500 HUNTSVILLE AL 35807-3801
1	OFC OF THE PRODUCT MGR SFAE AR HIP IP R DE KLEINE PICATINNY ARSENAL NJ 07806-5000
1	PM CRUSADER MUNITIONS SFAE GCSS CRM LTC D ARMOUR BLDG 171A PICATINNY ARSENAL NJ 07806-5000
1	CDR US ARMY ARDEC PROD BASE MODRNZTN AGENCY AMSMC PBM A SIKLOSI PICATINNY ARSENAL NJ 07806-5000
1	CDR US ARMY ARDEC PROD BASE MODRNZTN AGENCY AMSTA AR WES L LAIBSON PICATINNY ARSENAL NJ 07806-5000

NO. OF COPIES	ORGANIZATION
3	PM PEO ARMAMENTS TANK MAIN ARMAMENT SYS AMCPM TMA AMCPM TMA 105 AMCPM TMA AS H YUEN PICATINNY ARSENAL NJ 07806-5000
2	CDR US ARMY ARDEC AMSTA AR CCH B C MANDALA E FENNELL PICATINNY ARSENAL NJ 07806-5000
1	CDR US ARMY ARDEC AMSTA AR CCS PICATINNY ARSENAL NJ 07806-5000
1	CDR US ARMY ARDEC AMSTA AR WE D DOWNS PICATINNY ARSENAL NJ 07806-5000
1	COMMANDER US ARMY ARDEC AMSTA AR CCH P J LUTZ PICATINNY ARSENAL NJ 07806-5000
3	CDR US ARMY ARDEC AMSTA AR AEE WW M MEZGER D WIEGAND P LU PICATINNY ARSENAL NJ 07806-5000
1	CDR US ARMY ARDEC AMSTA AR DBS T G FERDINAND PICATINNY ARSENAL NJ 07806-5000

NO. OF COPIES	ORGANIZATION
10	CDR US ARMY ARDEC AMSTA AR WEE M PADUANO S EINSTEIN S WESTLEY S BERNSTEIN J RUTKOWSKI B BRODMAN P O'REILLY R CIRINCIONE P HUI J O'REILLY PICATINNY ARSENAL NJ 07806-5000
1	COMMANDER AMSTA AR FS T GORA PICATINNY ARSENAL NJ 07806-5000
1	CDR US ARMY ARDEC AMSTA AR FS DH PICATINNY ARSENAL NJ 07806-5000
2	CDR US ARMY ARDEC AMSTA AR FSA S R KOPMANN B MACHAK PICATINNY ARSENAL NJ 07806-5000
1	CDR US ARMY ARDEC AMSTA AR FSA D K CHUNG PICATINNY ARSENAL NJ 07806-5000
1	DIR BENET WEAPONS LAB AMSTA AR CCB T S SOPOK WATERVLIET NY 12189-4050
1	DIR BENET WEAPONS LAB AMSTA AR CCB TA M AUDINO WATERVLIET NY 12189-4050

NO. OF COPIES	ORGANIZATION
1	DIR BENET WEAPONS LAB AMSTA AR CCB D R HASENBEIN WATERVLIET NY 12189-4050
2	CDR US ARMY RSRCH OFC TECH LIB D MANN PO BOX 12211 RESEARCH TRIANGLE PARK NC 27709-2211
1	PM US TANK AUTOMOTIVE CMD AMCPM ABMS T DEAN WARREN MI 48092-2498
1	PM US TANK AUTOMOTIVE CMD FIGHTING VEHICLES SYSTEMS SFAE ASM BV WARREN MI 48397-5000
1	PM ABRAMS TANK SYSTEM SFAE ASM AB WARREN MI 48397-5000
1	DIR HQ TRAC RPD ATCD MA FT MONROE VA 23651-5143
1	COMMANDER RADFORD ARMY AMMUNITION PLANT SMCAR QA HI LIB RADFORD VA 24141-0298
1	COMMANDER US ARMY NGIC AMXST MC 3 220 SEVENTH ST NE CHARLOTTESVILLE VA 22901-5396
1	COMMANDANT USAFAC&S ATSF CD COL T STRICKLIN FT SILL OK 73503-5600
1	COMMANDANT USAFC&S ATSF CN P GROSS FT SILL OK 73503-5600

NO. OF COPIES	ORGANIZATION
4	CDR NAVAL RSRCH LAB TECH LIBRARY CODE 4410 K KAILASANATE J BORIS E ORAN WASHINGTON DC 20375-5000
1	OFFICE OF NAVAL RSRCH CODE 473 J GOLDWASSER 800 N QUINCY ST ARLINGTON VA 22217-9999
1	OFFICE OF NAVAL TECHLGY ONT 213 D SIEGEL 800 N QUINCY ST ARLINGTON VA 22217-5000
6	CDR NAVAL SURFACE WARFARE CTR T C SMITH S MITCHELL S PETERS J CONSAGA C GOTZMER TECH LIB INDIAN HEAD MD 20640-5000
1	CDR NAVAL SURFACE WARFARE CTR CODE G30 GUNS & MUNITIONS DIV DAHLGREN VA 22448-5000
1	CDR NAVAL SURFACE WARFARE CTR CODE G32 GUNS SYSTEMS DIV DAHLGREN VA 22448-5000
1	CDR NAVAL SURFACE WARFARE CTR CODE E23 TECH LIB DAHLGREN VA 22448-5000
1	CDR NAVAL SURFACE WARFARE CTR R HUBBARD DAHLGREN VA 22448-5000

NO. OF COPIES	ORGANIZATION
2	CDR NAVAL AIR WARFARE CTR CODE 388 C F PRICE T BOGGS CHINA LAKE CA 93555-6001
2	CDR NAVAL AIR WARFARE CTR CODE 3895 T PARR R DERR CHINA LAKE CA 93555-6001
1	CDR NAVAL AIR WARFARE CTR INFORMATION SCIENCE DIV CHINA LAKE CA 93555-6001
1	WL MNME ENERGETIC MATERIALS BR 2306 PERIMETER RD STE 9 EGLIN AFB FL 32542-5910
2	HQ DTRA D LEWIS A FAHEY 6801 TELEGRAPH RD ALEXANDRIA VA 22310-3398
1	DIR SANDIA NATL LABS M BAER DEPT 1512 PO BOX 5800 ALBUQUERQUE NM 87185
1	DIR SANDIA NATL LABS R CARLING COMBUSTION RSRCH FACILITY LIVERMORE CA 94551-0469
2	DIR LLNL L 355 A BUCHINGHAM M FINGER PO BOX 808 LIVERMORE CA 94550-0622

NO. OF COPIES	ORGANIZATION
2	BATTELLE TWSTIAC V LEVIN 505 KING AVE COLUMBUS OH 43201-2693
1	BATTELLE PNL M GARNICH PO BOX 999 RICHLAND WA 99352
1	MCELROY AND ASSOCIATES CAGE 1CKS9 H A MCELROY 7227 ALAFIA RIDGE LOOP RIVERVIEW FL 33569-4702
1	CPI JHU H J HOFFMAN 10630 LITTLE PATUXENT PKWY STE 202 COLUMBIA MD 21044-3200
1	AFELM THE RAND CORP LIBRARY D 1700 MAIN ST SANTA MONICA CA 90401-3297
1	BRIGHAM YOUNG UNIV M BECKSTEAD DEPT OF CHEMICAL ENGRG PROVO UT 84601
1	CALIF INSTITUTE OF TECHLGY F E C CULICK 204 KARMAN LAB MAIN STOP 301 46 1201 E CALIFORNIA ST PASADENA CA 91109
1	MILLERSVILLE UNIV PHYSICS DEPT C W PRICE MILLERSVILLE PA 17551
2	UNIV OF ILLINOIS DEPT OF MECH INDUSTRY ENGRG H KRIER R BEDDINI 144 MEB 1206 N GREEN ST URBANA IL 61801-2978
1	UNIV OF MASSACHUSETTS DEPT OF MECHANICAL ENGRG K JAKUS AMHERST MA 01002-0014
1	UNIV OF MINNESOTA DEPT OF MECHANICAL ENGRG E FLETCHER MINNEAPOLIS MN 55414-3368
4	PENNSYLVANIA STATE UNIV DEPT OF MECHANICAL ENGRG V YANG K KUO S THYNELL G SETTLES UNIVERSITY PARK PA 16802-7501
1	RUTGERS UNIVERSITY DEPT OF MECH AND AERO ENGRG S TEMKIN UNIV HEIGHTS CAMPUS NEW BRUNSWICK NJ 08903
1	UNIV OF UTAH DEPT OF CHEMICAL ENGRG A BAER SALT LAKE CITY UT 84112-1194
1	ARROW TECHLGY ASSOC INC 1233 SHELBURNE RD D 8 SOUTH BURLINGTON VT 05403
1	AAI CORPORATION D CLEVELAND PO BOX 126 HUNT VALLEY MD 21030-0126

NO. OF COPIES	ORGANIZATION
7	ALLIANT TECHSYSTEMS INC R E TOMPKINS J BODE C CANDLAND L OSGOOD R BURETTA R BECKER M SWENSON 600 SECOND ST NE HOPKINS MN 55343
1	ELI FREEDMAN AND ASSOC E FREEDMAN 2411 DIANA RD BALTIMORE MD 21209-1525
2	ALLIANT TECHSYSTEMS INC W B WALKUP T F FARABAUGH ALLEGHENY BALLISTICS LAB PO BOX 210 ROCKET CENTER WV 26726
6	ALLIANT TECHSYSTEMS INC L GIZZI D A WORRELL W J WORRELL C CHANDLER S RITCHIE A ZEIGLER RADFORD ARMY AMMO PLANT RADFORD VA 24141-0299
1	ALLIANT TECHSYSTEMS INC R CARTWRIGHT AEROSPACE 100 HOWARD BLVD KENVILLE NJ 07847
1	L MARTIN ARM SYS J TALLEY RM 1309 LAKESIDE AVE BURLINGTON VT 05401
1	PRIMEX F E WOLF BADGER ARMY AMMO PLANT BARABOO WI 53913
3	PRIMEX E J KIRSCHKE A F GONZALEZ J DRUMMOND D W WORTHINGTON PO BOX 222 SAINT MARKS FL 32355-0222
2	PRIMEX N HYLTON J BUZZETT 10101 9TH ST NORTH ST PETERSBURG FL 33716
1	PAUL GOUGH ASSOC INC P S GOUGH 1048 SOUTH ST PORTSMOUTH NH 03801-5423
1	FRELIN ASSOCIATES INC 4411 QUAKER HILLS CT HAVRE DE GRACE MD 21078
1	GEN DYN DEF SYS (PCRL) N MESSINA PRINCETON CORPORATE PLAZA 11 DEERPARK DR BLDG IV STE 119 MONMOUTH JUNCTION NJ 08852
2	ROCKWELL INTRNTNL SCIENCE CTR DR S CHAKRAVARTHY DR S PALANISWAMY 1049 CAMINO DOS RIOS PO BOX 1085 THOUSAND OAKS CA 91360
1	KELLER CONSULTING INC G KELLER 265 CHARLOTTE ST #10 ASHEVILLE NC 28801-1400
1	SOUTHWEST RSRCH INST J P RIEGEL 6220 CULEBRA RD PO DRAWER 28510 SAN ANTONIO TX 78228-0510

NO. OF COPIES	ORGANIZATION
3	VERITAY TECHGY INC E FISHER R SALIZONI J BARNES 4845 MILLERSPORT HWY EAST AMHERST NY 14501-0305
1	PRIMEX E STEINER DIR LARGE CAL R&D PO BOX 127 RED LION PA 17356
1	SRI INTERNATIONAL TECH LIB PROPULSION SCIENCES DIV 333 RAVENWOOD AVE MENLO PARK CA 94025-3493

NO. OF COPIES	ORGANIZATION
	ABERDEEN PROVING GROUND
1	CDR USAATC STECS LI R HENDRICKSEN
27	DIR USARL AMSRL WM B RINGERS AMSRL WM B A HORST AMSRL WM BE T MINOR T COFFEE C LEVERITT W OBERLE L M CHANG J COLBURN P CONROY D KOOKER M NUSCA AMSRL WM BC P PLOSTINS M BUNDY B GUIDOS D LYON J GARNER V OSKAY P WEINACHT AMSRL WM BD M MCQUAID B FORCH C CHABALOWSKI AMSRL WM MC J MONTGOMERY J BEATTY R ADLER AMSRL WM MB L BURTON AMSRL CI HA W STUREK AMSRL CI C NIETUBICZ

INTENTIONALLY LEFT BLANK.

REPORT DOCUMENTATION PAGE

Form Approved
OMB No. 0704-0188

Public reporting burden for this collection of information is estimated to average 1 hour per response, including the time for reviewing instructions, searching existing data sources, gathering and maintaining the data needed, and completing and reviewing the collection of information. Send comments regarding this burden estimate or any other aspect of this collection of information, including suggestions for reducing this burden, to Washington Headquarters Services, Directorate for Information Operations and Reports, 1215 Jefferson Davis Highway, Suite 1204, Arlington, VA 22202-4302, and to the Office of Management and Budget, Paperwork Reduction Project(0704-0188), Washington, DC 20503.

1. AGENCY USE ONLY *(Leave blank)*	2. REPORT DATE	3. REPORT TYPE AND DATES COVERED
	May 2001	Final, February–December 1998

4. TITLE AND SUBTITLE
Extended-Range 5-in Navy Gun: Theoretical Thermal and Erosion Investigations

5. FUNDING NUMBERS
622618AH80

6. AUTHOR(S)
Paul J. Conroy, Paul Weinacht, Michael J. Nusca, and Kirk Rice*

7. PERFORMING ORGANIZATION NAME(S) AND ADDRESS(ES)
U.S. Army Research Laboratory
ATTN: AMSRL-WM-BE
Aberdeen Proving Ground, MD 21005-5066

8. PERFORMING ORGANIZATION REPORT NUMBER
ARL-TR-2473

9. SPONSORING/MONITORING AGENCY NAMES(S) AND ADDRESS(ES)

10.SPONSORING/MONITORING AGENCY REPORT NUMBER

11. SUPPLEMENTARY NOTES
*Formerly of the U.S. Naval Surface Warfare Center, Indian Head, MD 20640-5035

12a. DISTRIBUTION/AVAILABILITY STATEMENT
Approved for public release; distribution is unlimited.

12b. DISTRIBUTION CODE

13. ABSTRACT*(Maximum 200 words)*

Barrel heating and erosion concerns for the Navy are being brought to light by new extended-range munitions. These munitions have, in general, higher performance requirements and use new propellants. In light of these concerns, the following investigation was performed to determine the thermal and erosion characteristics of the current and proposed munitions. In this report, the calculation methodology governing both the thermal and erosion work is described. Six thermal scenarios were computed to compare the thermal load from various combinations of charges. Single-shot erosion predictions are presented for three charges: MK67 with NACO propellant, MK73 with M30A1 propellant, and EX167 extended-range guided munitions (ERGM) propelling charge with EX99 propellant. A fourth single-shot erosion calculation was made using the product gas-state variables and gas velocity of the MK73 charge with chemical constituents of EX99 propellant. The erosion results highlight propellant combustion product differences at the surface between the current and newer propellants. The primary conclusion is that carburization leading to iron carbide formation may be an important contributing factor for much of the material lost from the steel barrel once it is exposed through cracks or chips in the surface coating.

14. SUBJECT TERMS
gun tube erosion, erosion caused by nitramine propellant, gun tube heating, rapid fire cannons

15. NUMBER OF PAGES
33

16. PRICE CODE

17. SECURITY CLASSIFICATION OF REPORT	18. SECURITY CLASSIFICATION OF THIS PAGE	19. SECURITY CLASSIFICATION OF ABSTRACT	20. LIMITATION OF ABSTRACT
UNCLASSIFIED	UNCLASSIFIED	UNCLASSIFIED	UL

INTENTIONALLY LEFT BLANK.

USER EVALUATION SHEET/CHANGE OF ADDRESS

This Laboratory undertakes a continuing effort to improve the quality of the reports it publishes. Your comments/answers to the items/questions below will aid us in our efforts.

1. ARL Report Number/Author ARL-TR-2473 (Conroy) Date of Report May 2001

2. Date Report Received _____

3. Does this report satisfy a need? (Comment on purpose, related project, or other area of interest for which the report will be used.) _____

4. Specifically, how is the report being used? (Information source, design data, procedure, source of ideas, etc.) _____

5. Has the information in this report led to any quantitative savings as far as man-hours or dollars saved, operating costs avoided, or efficiencies achieved, etc? If so, please elaborate. _____

6. General Comments. What do you think should be changed to improve future reports? (Indicate changes to organization, technical content, format, etc.) _____

CURRENT ADDRESS

_____
Organization

_____
Name E-mail Name

_____
Street or P.O. Box No.

_____
City, State, Zip Code

7. If indicating a Change of Address or Address Correction, please provide the Current or Correct address above and the Old or Incorrect address below.

OLD ADDRESS

_____
Organization

_____
Name

_____
Street or P.O. Box No.

_____
City, State, Zip Code

(Remove this sheet, fold as indicated, tape closed, and mail.)
(DO NOT STAPLE)